

Broadband CPW-Fed Circularly Polarized Planar Monopole Antenna with Inverted-L Strip and Asymmetric Ground Plane for WLAN Application

Qiang Chen^{1, *}, Hou Zhang¹, Luchun Yang², Bin Xue¹, and Xueliang Min¹

Abstract—A novel broadband circularly polarized planar monopole antenna fed by coplanar waveguide (CPW) is proposed and fabricated. The proposed antenna consists of a rectangular monopole, an inverted-L strip and an asymmetric ground plane with cutting a horizontal slit on the right ground plane. Firstly, a narrow circularly polarized (CP) radiation at the upper band can be achieved by utilizing the asymmetric ground plane. Then, an inverted-L strip is introduced to obtain broadband CP characteristic matched with wide impedance bandwidth. The measured results demonstrate that a 10-dB bandwidth of 58.8% from 4.8 to 8.8 GHz and a 3-dB axial-ratio bandwidth (ARBW) of 47.8% from 5.375 to 8.75 GHz can be achieved which can completely cover the WLAN (5.725–5.85 GHz) band. Additionally, a 10-dB impedance bandwidth of 24% (3.3–4.2 GHz) with linear polarization is also obtained which can completely cover the WiMAX (3.3–3.7 GHz) bands. In addition, to explain the mechanism of dual-band CP operation, the analysis of magnetic fields distributions and a parametric study of the design are given. Compared to other recent works, a simpler structure, wider axial ratio and impedance bandwidths and a more compact size are the key features of the proposed antenna.

1. INTRODUCTION

Nowadays, circular polarization technique has been widely used in the fields of communication and electronic countermeasure. Also mitigating the depolarizing effect of the transmission channel with a higher reliability ensured has found applications in circularly polarized antennas. Moreover, with advantages of resistance to bad weather conditions and immunity to multipath propagation, more attentions have been attracted for applications in diverse area for circularly polarized antennas. Circular polarization (CP) can be achieved, when two degenerate modes of phase difference of 90 degrees, but equal amplitudes are excited. In the past few years, due to the advantages of low profile, low cost, broadband operating bandwidths and simple structure in comparison to a microstrip feed for the design of active-integrated antennas, printed monopole antennas fed by CPW are advantageous for feeding arrangements and various structures proposed for CP. As listed in [1–3], some of the circular polarization antennas based on CPW-Fed are discussed and then analyzed.

To achieve CP radiation, several printed monopole antennas have been proposed [4–10]. Linearly polarized (LP) and CP operations were achieved by a multi-band coplanar monopole antenna with the trapezoidal structure adopted in [4]. A structure of the asymmetrical ground plane in [5] was used to excite a CP operation at 1.57 GHz with the width of the CPW ground plane adjusted simply. As reported in [6], a CP operation was introduced by two arms with different lengths in a simple printed monopole. In addition, with using slots in the ground [7], four notch slots [8], feed positioning with U-

Received 12 February 2017, Accepted 28 April 2017, Scheduled 21 May 2017

* Corresponding author: Qiang Chen (cqky1989@126.com).

¹ Air and Missile Defense College, Air Force Engineering University, Xi'an, Shaanxi Province 710051, China. ² China Mobile (Shenzhen) Limited, Shenzhen, Guangdong Province 518048, China.

and E-shaped slots [9], slotted monopole [10], S-shaped slots [11], inverted L-slits on the ground and feed networks composed of three Wilkinson power dividers [12] included, a great effort was revealed in implementing various techniques for obtaining circularly polarized monopole antennas. But due to the narrow CP bandwidth among them, several wideband CP monopole antennas were proposed in [13–16]. In [13], a slot monopole antenna with a power division network employed was adopted, and a 30% AR (axial ratio) bandwidth was achieved by adjusting the size of slot, which led to a large size and complex geometry instead. Thus, compact size plays a great role in applicability of the final design in CP antenna. By parallel-aligning an inverted L-shaped strip and cutting an inverted L-shaped slot on the ground plane in [14], a CP bandwidth larger than 30% could be achieved.

Meanwhile, broadband CP radiation could be also produced by moon-shaped [15] or chifre-shaped [16] monopole antennas. However, due to ground planes with slots and stubs, or embedded, complex structures and large size adopted in most of the broadband CP monopole antennas in [13–16], designing a planar monopole with a simple structure, compact size and wide AR width is desirable.

In this paper, a novel broadband CPW-fed circularly polarized planar monopole antenna with inverted-L strip and asymmetric ground plane for WLAN application is proposed. By combining the inverted-L strip and asymmetric ground plane with two adjacent CP modes coupled together, a broad 3-dB AR bandwidth can be achieved. Simulated results have shown that the proposed antenna can achieve a 10-dB impedance bandwidth of 58.8% (4.8–8.8 GHz) and an axial ratio bandwidth of 47.8% (5.375–8.75 GHz). Additionally, linear polarization with the 10-dB impedance bandwidth of 24% (3.3–4.2 GHz) which can completely cover the WiMAX (3.3–3.7 GHz) band can also be achieved. Compared with recently published antennas, a simpler structure, broadband axial ratio, wider impedance matching and more compact size can be obtained.

2. ANTENNA STRUCTURE

2.1. Antenna Configuration

The geometry of the proposed CPW-fed monopole antenna is depicted in Fig. 1(a). The proposed antenna is printed on an FR4 substrate with a dielectric constant of 4.4, loss tangent of 0.02 and

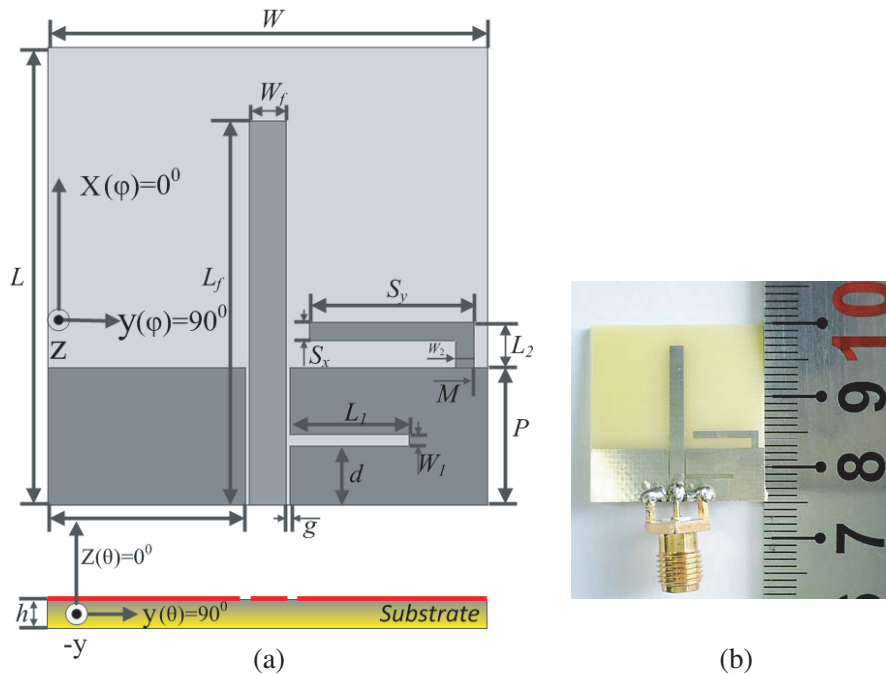


Figure 1. Structure of the proposed CPW-Fed planar monopole antenna and its prototype. (a) Configuration of antenna structure, (b) fabricated prototype of the Proposed antenna.

dimension of $W \times L \times h$. The antenna is fed by a CPW line with 50 ohms characteristic impedance, characterized by a size of $L_f \times W_f$ and gaps on both sides with width g .

Based on the structure of Ant. 1, an asymmetric ground plane with a slit etched on the right part is introduced to excite upper band CP operation, and good impedance match is obtained. To obtain an additional CP mode and widen impedance bandwidth, an inverted-L strip on the ground plane is employed on the basis of asymmetric ground and monopole radiator. Then, broadband CP can be obtained with two adjacent CP modes combined by adjusting the size of inverted-L strip and length of the slit etched on the ground plane. According to the simulation studies from ANSYS HFSS 13, to achieve maximized 3-dB AR bandwidth while keeping the return loss better than 10 dB, the dimensions of the inverted-L strip, the slit and CPW feed line are optimized which are shown in details in Table 1.

Table 1. Optimal dimensions of the proposed antenna.

Dimension	Size (mm)	Dimension	Size (mm)
L	25	S_y	9
W	24	d	3.5
h	1	W_2	1
P	7.5	M	0.75
W_f	2	g	0.2
L_f	22	L_1	6.5
S_x	1	L_2	1.5

2.2. Operating Principle

As depicted in Fig. 2, three prototypes (Ant. 1 to Proposed Antenna) are displayed to understand the operating principle of the designed antenna. Also the performances of S_{11} and AR in Ant. 1, Ant. 2 and the proposed antenna are compared. As shown in Fig. 3, a fundamental resonant mode at 4 GHz is generated by a conventional CPW-Fed monopole Ant. 1. It is generally known that due to the weak radiation in vertical direction, CP radiation is difficult to be generated for a traditional monopole which can be explained by the magnetic field vectors in Fig. 4. Obviously, as displayed in Fig. 4(a), the vertical directions of the magnetic field vectors of two ground planes are opposite which means that due to the small vertical components, horizontal polarization radiation can be achieved with the vertical magnetic field vectors counteracted. Thus, linear polarization is produced with a large value of AR shown in Fig. 3. So an asymmetric ground plane is employed to generate two orthogonal modes with a 90-degree phase difference. As shown in Fig. 4(b), a vertical component is produced by an asymmetric ground plane in which vertical magnetic field vectors are yielded at the right ground plane in Ant. 2. Due to the employment of asymmetric ground plane, a narrow CP bandwidth between 7.4–8.5 GHz and an additional resonant mode at 6 GHz can be achieved simultaneously. But the antenna cannot possess broadband CP property in spite of the observed CP radiation. In order to achieve a broadband CP

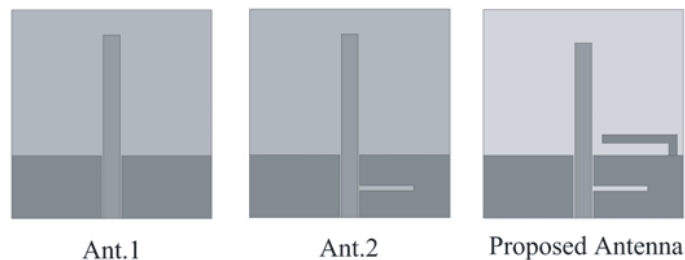


Figure 2. Three prototypes of the monopole antenna.

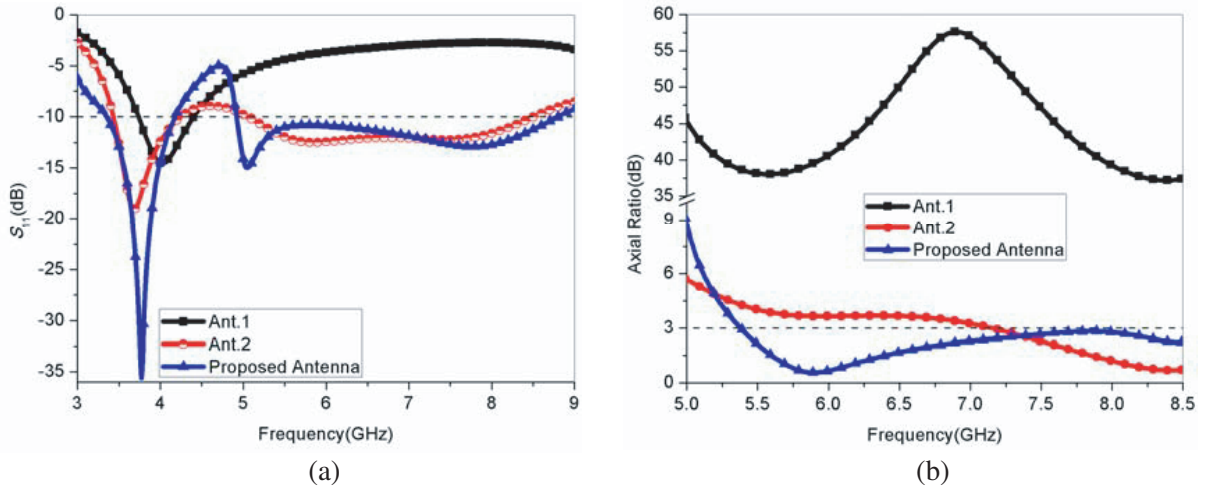


Figure 3. Simulated reflection coefficients and axial ratio in comparison with different monopole antennas. (a) S_{11} , (b) AR.

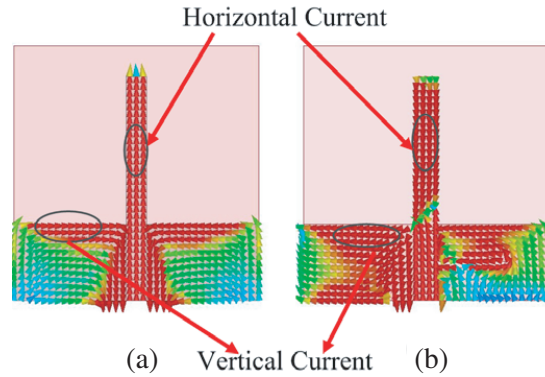


Figure 4. Simulated surface current distributions. (a) Ant. 1 at 3.26 GHz, (b) Ant. 2 at 7.8 GHz.

radiation, inverted-L strip is embedded in the right corner of the asymmetric ground plane. As depicted in Fig. 3, an additional CP radiation generated at 5.8 GHz can be achieved with the employment of the coupled effect between inverted-L strip and asymmetric ground plane. As we know, additional vertical components can be produced due to inverted-L strip embedded, and so the lower band of CP operation can be introduced. Therefore, a broad CP performance is obtained by the lower CP band yielded by inverted-L strip which can be merged with the upper CP band mode, as revealed from Fig. 3. The AR and reflection coefficient bandwidth overlap with each other perfectly. Therefore, it can be concluded that from the comparison of results between the three antennas, the proposed antenna shows a wider impedance matching and wide CP radiation.

3. CIRCULAR POLARIZATION MECHANISM

As illustrated in Figs. 5(a)–(d), the simulated magnetic field vectors of the patches at 5.8 GHz for four different time phases instants, from 0° to 270° , with an interval of 90° are depicted, respectively. It can be observed that, as time varying, the magnetic field vectors rotate mainly in the direction of anticlockwise, which means that the right-handed circular polarization (RHCP) operation is produced at 5.8 GHz, while as noticed, this RHCP operation is achieved at the direction of $z > 0$, located at the upper half space. Instead, a LHCP operation is observed at the $z < 0$ direction of the other half space.

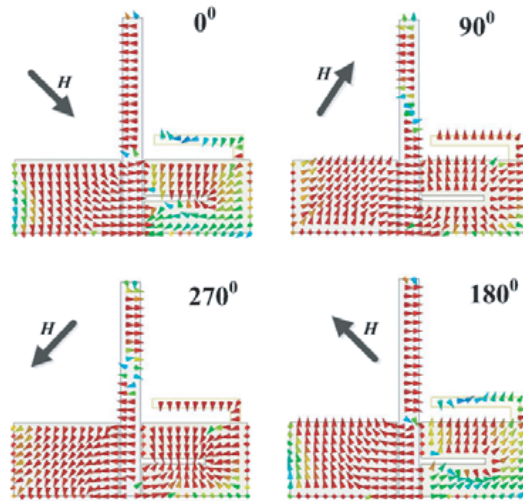


Figure 5. Magnetic fields distributions at 5.8 GHz.

4. PARAMETRIC STUDY AND DISCUSSION

To achieve good performance for broadband CP operation, different parameters adjustments have been simulated and then analyzed, where different impacts on the performance of the antenna will be found, so that the optimized dimensions of the monopole antenna could be got. So a slight modification of the antenna parameters for CP radiation should be required to achieve the desired AR bandwidth and impedance matching. Meanwhile, It is shown that a CP radiation mainly depend on dimensions of inverted-L strip, height of the ground plane and length of the slit which have been shown in Figs. 6(a) and (b). So the dimensions of inverted-L strip, height of the ground plane and length of the slit are especially analyzed and then simulated. The other optimized dimensions of parameters are listed in Table 1.

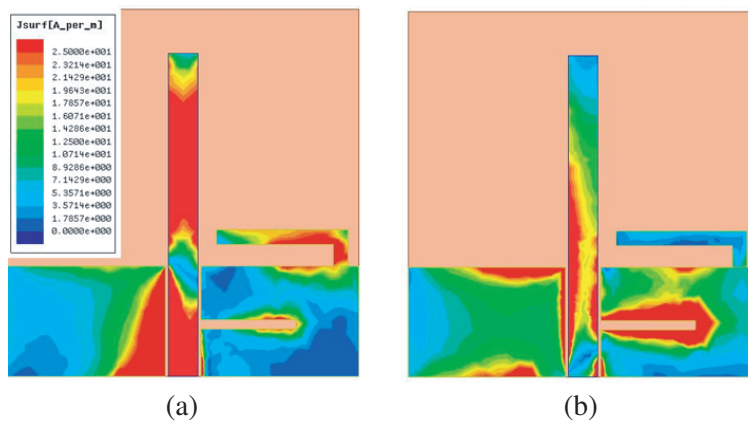


Figure 6. Surface current distributions of the proposed antenna. (a) 0°, (b) 90°.

4.1. The Effects of the L_1

As shown in Figs. 7(a) and (b), length of the slit, L_1 , is investigated to find its effect on the antenna performance. As demonstrated in Fig. 7, the variations of L_1 have great effects on the impedance operation. As L_1 increased, the first and second resonant frequency is shifted toward the lower and upper frequency, respectively. Meanwhile, the value of the $|S_{11}|$ at the middle band is deteriorated when

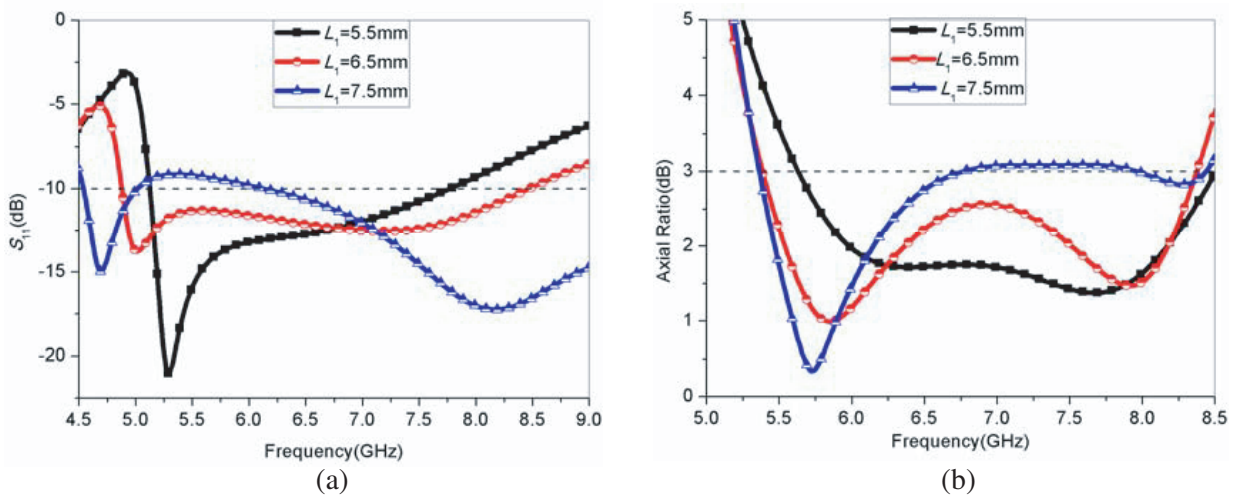


Figure 7. Effect of L_1 on antenna performance. (a) S_{11} , (b) AR.

L_1 increased. On the other hand, L_1 plays an important role on CP property of the antenna. As L_1 increases, the AR width is improved with little effects on the center frequency of AR curve. Thus, L_1 is selected as 6.5 mm.

4.2. The Effects of the S_y

The S_{11} and AR curves for various W_2 are displayed in Figs. 8(a) and (b). As observed in Fig. 8, when the length of inverted-L strip S_y increases, the first resonant frequency of the proposed antenna is shifted toward the lower frequency but little impact on the bandwidth of the reflection coefficient at the upper band. Meanwhile, both the first and the second CP mode shift to lower frequency as S_y varied from 8 mm to 10 mm. On the other hand, when S_y increases, the reflection coefficient remains unchanged at the upper band instead of the bandwidth of the AR shifted. So, to achieve a good performance in both the reflection coefficient and the AR, a tradeoff has to be made in selecting S_y . Thus, according to simulation and analysis the best impedance and AR property occurred for 9 mm.

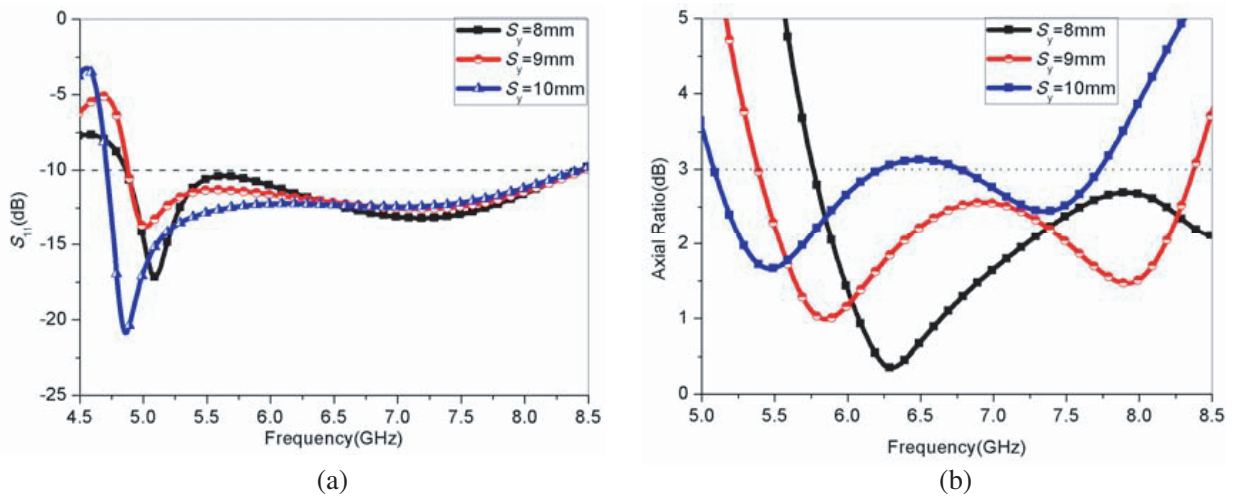


Figure 8. Effect of S_y on antenna performance. (a) S_{11} , (b) AR.

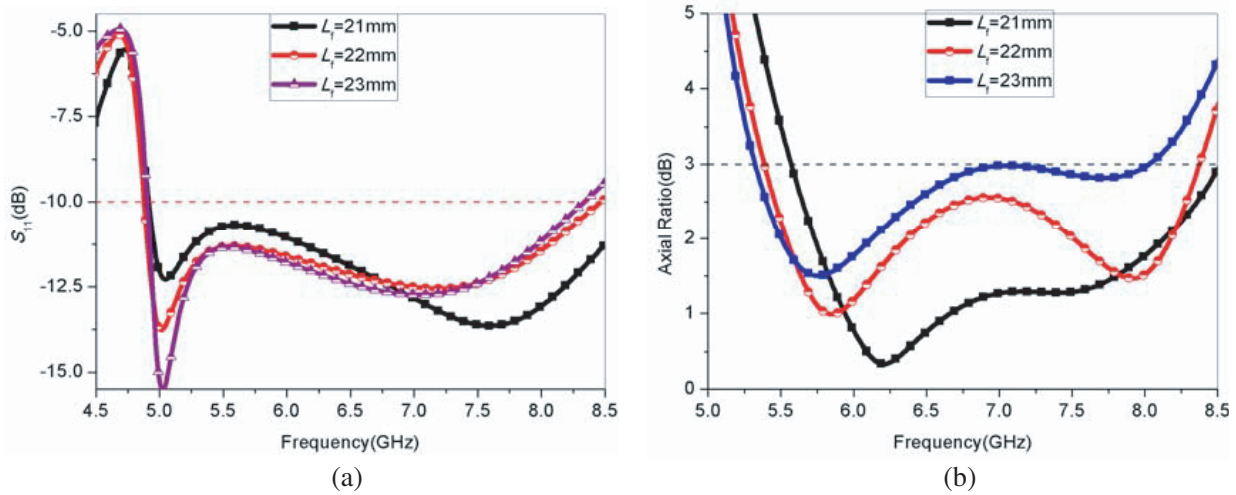


Figure 9. Effect of L_f on antenna performance. (a) S_{11} , (b) AR.

4.3. The Effects of the L_f

The S_{11} and AR curves for various L_f are displayed in Figs. 9(a) and (b). As observed in figures, better impedance matching is exhibited, and also the center frequency of the reflection coefficient is observed to increase as L_f varied from 21 mm to 23 mm with the upper resonant frequency shifted toward upper frequency. Meanwhile, it is shown that W_2 have great effect on the AR. For $L_f > 22$ mm, L_f increases with the CP radiation worsening rapidly which is unsatisfied for the desired CP bandwidth on the whole operation band instead of different performance when $L_f < 22$ mm. Moreover as depicted in Fig. 9(b), the CP performance is seen to lose when $L_f > 23$ mm at the upper band. Simulation and analysis show that the best impedance and AR property occurred for 22 mm.

5. SIMULATION AND MEASUREMENT RESULTS

In this framework, related semi-analytical techniques from [17–19] provide correct initial guesses for the optimization process which are considered to be used and cited. So as listed in Table 1, all the dimensions of the proposed antenna have been optimized according to the results of numerical analysis.

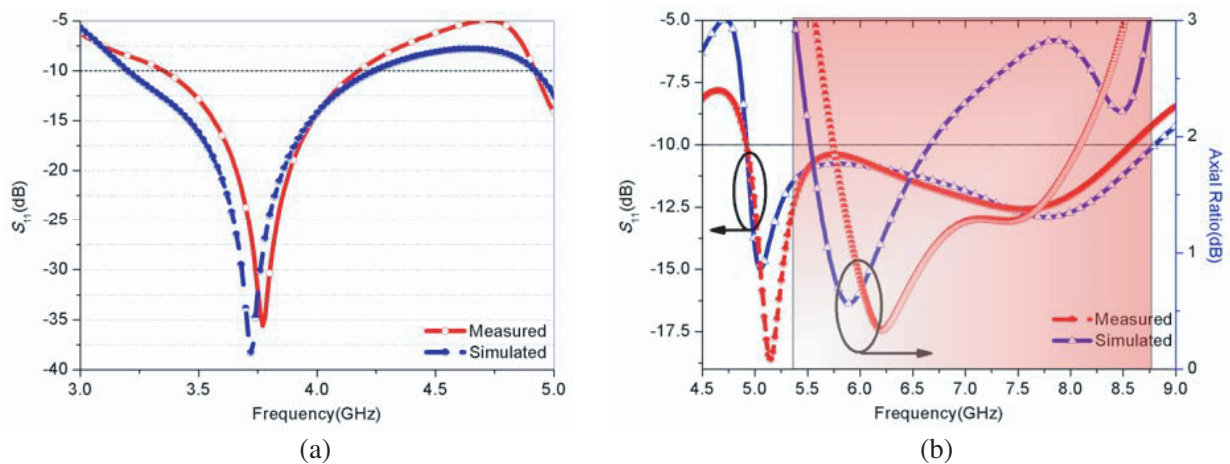


Figure 10. Simulated and measured reflection coefficients and axial ratio of the proposed antenna in the lower and upper band. (a) Lower band, (b) upper band.

The proposed antenna was initially simulated using HFSS and then fabricated with the optimized dimensions as shown in Fig. 1(b) with a photograph. Simulated and measured results of reflection coefficients and ARs of the proposed antenna are illustrated in Figs. 10(a) and (b). As can be seen from the figures, the simulated impedance bandwidth is 58.8% (4.8 to 8.8 GHz). It's shown that the measured CP bandwidths are 47.8%, ranging from 5.375 to 8.75 GHz at the center frequency of 7.06 GHz, which could completely cover the WLAN (5.725–5.85 GHz) band. An excellent agreement is observed between the simulated and measured $|S_{11}|$ and AR cures except for some mismatches which is contributed to the poor quality of the Sub Miniature version A(SMA) connector used and fabrication tolerance during

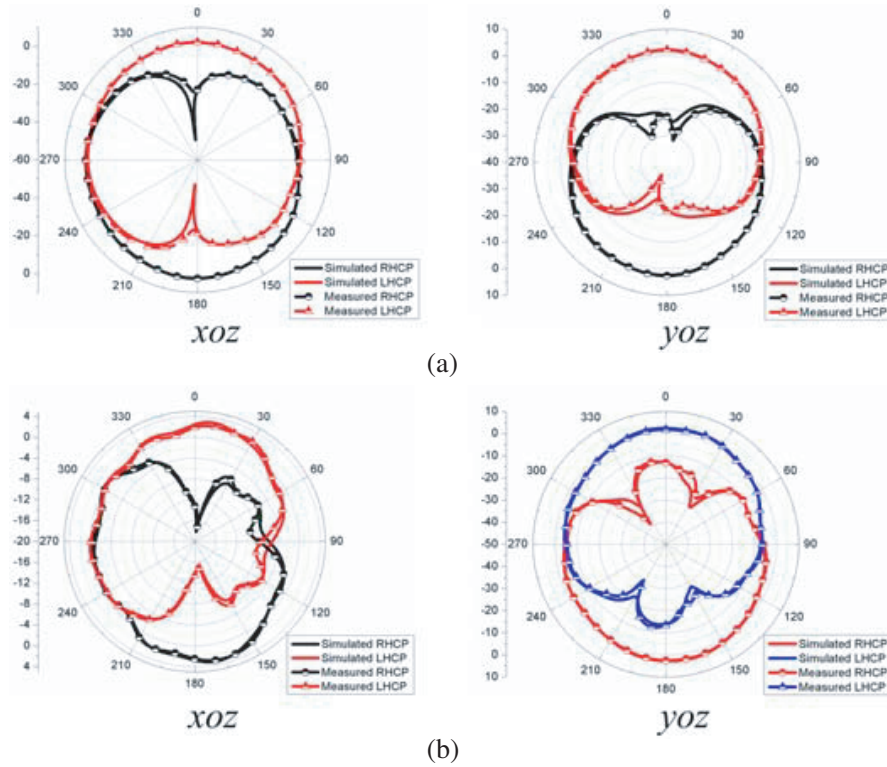


Figure 11. Simulated and measured radiation patterns in different planes. (a) 5.8 GHz, (b) 7.8 GHz.

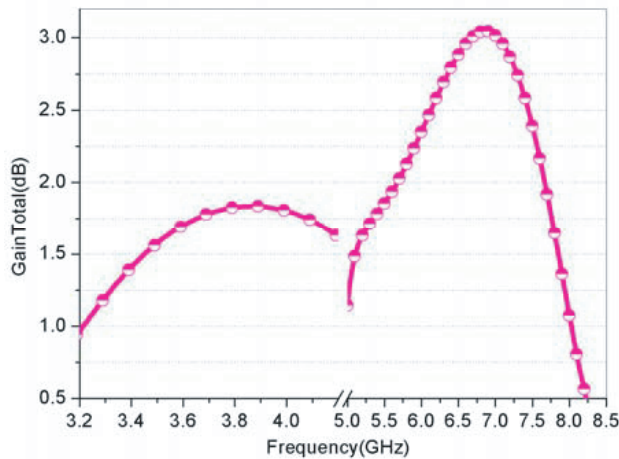


Figure 12. Measured gain of the proposed antenna.

measurements. Moreover, as observed in the figures, CP band is completely covered by impedance band.

From Figs. 11(a) and (b) we can see that compared with the measured radiation patterns in the E -plane (XZ plane, $\varphi = 0$) and H -plane (YZ plane, $\varphi = 90$), the simulated far-field radiation patterns of the antenna are validated. Clearly, left-hand circularly polarized (LHCP) and right-hand circularly polarized (RHCP) radiation patterns depend on whether in $+Z$ direction (upper hemisphere) or $-Z$ direction (lower hemisphere) you observe. In addition, from Figs. 11(a) and (b), it can be apparently observed that the simulated and measured patterns agree well with each other, which is proved in the performance of the antenna design. Meanwhile, the measured peak gains are 1.8 dB and 3.4 dB, shown in Fig. 12. Moreover, as listed in Table 2, compared to the recent wideband CP antenna, a better gain performance is characterized at CP bandwidths in spite of the deterioration out of the CP bandwidth.

Table 2. Comparison of different structures presented in literatures.

Structures	10-dB S_{11} BW (%)	3-dB ARBW (%)	Antenna Size (mm)
Presented in [13]	78.1% (4.1 GHz)	43% (2.54 GHz)	$70 \times 50 \times 3.2$
Presented in [14]	40% (2.4 GHz)	31.8% (1.95 GHz) (5.15–7.11 GHz)	$20 \times 20 \times 0.813$
Presented in [15]	49.7% (1.49 GHz)	39% (1.48 GHz)	$70 \times 46.6 \times 0.8$
Presented in [16]	75% (2.4 GHz)	41.6% (2.5 GHz)	$63 \times 58.4 \times 1.5$
Presented in [20]	40% (6 GHz)	33% (1.59 GHz)	$70 \times 70 \times 1.6$
Proposed Antenna	24% (0.9 GHz)	47.8% (3.375 GHz) (5.375–8.75 GHz)	$25 \times 24 \times 1$
	56.9% (3.9 GHz)		

6. CONCLUSIONS

In this paper, a novel broadband CPW-fed circularly polarized planar monopole antenna is presented. A broad 3-dB AR bandwidth can be produced by combining inverted-L strip and asymmetric ground plane with two adjacent CP modes coupled together. Simulated results show that the proposed antenna can achieve a 10-dB impedance bandwidth of 58.8% (4.88.8 GHz) and an axial ratio bandwidth of 47.8% (5.375–8.75 GHz) which have a good agreement with measured data. In addition, linear polarization with the 10-dB impedance bandwidth of 24% (3.3–4.2 GHz) can also be achieved. To achieve good performances for wide CP radiation, a series of parameter adjustments have been made to optimize the design. Simulated and measured results show that a simpler structure, broadband axial ratio, wider impedance matching and more compact size than recently published antennas can be obtained.

REFERENCES

1. Sze, J. Y., C. I. G. Hsu, Z. W. Chen, and C. C. Chang, "Broadband CPW-fed circularly polarized square slot antenna with lightning-shaped feed line and inverted-L grounded strips," *IEEE Trans. Antennas Propag.*, Vol. 58, No. 3, 973–977, 2010.
2. Liu, Y. W. and P. Hsu, "Broadband circularly polarized square slot antenna fed by co-planar waveguide," *Electron. Lett.*, Vol. 49, No. 16, 976–977, 2013.
3. Chen, Y. B., Y. C. Jiao, and F. S. Zhang, "Polarization reconfigurable cpw-fed square slot antenna using pin diodes," *Microw. Opt. Technol. Lett.*, Vol. 49, No. 6, 1233–1236, 2007.
4. Augustin, G. and T. A. Denidni, "Coplanar waveguide-fed uniplanar trapezoidal antenna with linear and circular polarization," *IEEE Trans. Antennas Propag.*, Vol. 60, No. 5, 2522–2526, May 2012.
5. Wang, C. J. and K. L. Hisao, "CPW-fed monopole antenna for multiple system integration," *IEEE Trans. Antennas Propag.*, Vol. 62, No. 2, 1007–1011, Feb. 2014.

6. Ghobadi, A. and M. Dehmollaian, "A printed circularly polarized Y-shaped monopole antenna," *IEEE Antennas Wireless Propag. Lett.*, Vol. 11, 22–25, 2012.
7. Li, G., H. Zhai, T. Li, L. Li, and C. Liang, "A compact antenna with broad bandwidth and quad-sense circular polarization," *IEEE Antennas Wireless Propag. Lett.*, Vol. 11, 791–794, 2012.
8. Ren, H., Y. Yu, and Z. Shen, "Broadband circularly-polarized antenna consisting of four notch slot radiators," *Electron. Lett.*, Vol. 48, No. 23, 1447–1449, Nov. 2012.
9. Chen, Y. and C. Wang, "Characteristic-mode-based improvement of circularly polarized U-slot and E-shaped patch antennas," *IEEE Antennas Wireless Propag. Lett.*, Vol. 11, 1474–1477, 2012.
10. Rezaeieh, S. A. and A. Abbosh, "Broadband CPW-fed slot antenna with circular polarization for on-body applications at ISM band," *Proc. Asia-Pacific Microw. Conf.*, 1184–1186, Dec. 4–7, 2012.
11. Li, G., H. Zhai, T. Li, L. Li, and C. Liang, "CPW-fed S-shaped slot antenna for broadband circular polarization," *IEEE Antennas Wireless Propag. Lett.*, Vol. 12, 619–622, 2013.
12. Hu, Y. J., W. P. Ding, W. M. Ni, and W. Q. Cao, "Broadband circularly polarized cavity-backed slot antenna array with four linearly polarized disks located in a single circular slot," *IEEE Antennas Wireless Propag. Lett.*, Vol. 11, 496–499, 2012.
13. Kumar, T. and A. R. Harish, "Broadband circularly polarized printed slot-monopole antenna," *IEEE Antennas Wireless Propag. Lett.*, Vol. 12, 1531–1534, 2013.
14. Ahdi Rezaeieh, S., A. Abbosh, and M. A. Antoniadis, "Compact CPW-fed planar monopole antenna with wide circular polarization bandwidth," *IEEE Trans. Antennas Propag.*, Vol. 12, 1295–1298, 2013.
15. Hu, B., Nasimuddin, and Z. Shen, "Moon-shaped printed monopole antenna for wideband circularly polarized radiation," *Proc. IEEE-APS Topical Conf. on Antennas and Propagation in Wireless Communications (APWC)*, 825–827, 2013.
16. Han, R. C. and S. S. Zhong, "Broadband circularly-polarized chifre-shaped monopole antenna with asymmetric feed," *Electron. Lett.*, Vol. 52, No. 4, 256–258, Feb. 2016.
17. Chang, H.-W. and S.-Y. Mu, "Semi-analytical solutions of the 3-D homogeneous Helmholtz Equation by the method of connected local fields," *Progress In Electromagnetics Research*, Vol. 142, 159–188, 2013.
18. Sen, S. G., "A semi-analytical method to calculate the entries of the method of moments matrix for the mixed potential integral equation of a source reconstruction problem," *Progress In Electromagnetics Research M*, Vol. 41, 149–158, 2015.
19. Li, Y. L. and S. Sun, "Full-wave semi-analytical modeling of planar spiral inductors in layered media," *Progress In Electromagnetics Research*, Vol. 149, 45–54, 2014.
20. Yang, S. L. S., A. A. Kishk, and K. F. Lee, "Wideband circularly polarized antenna with L-shaped slot," *IEEE Trans. Antennas Propag.*, Vol. 56, No. 6, 1780–1783, Jun. 2008.